SPRINGER NATURE Link

Find a journal | Publish with us | Track your research | Search

Home > Virchows Archiv > Editorial board



Virchows Archiv
European Journal of Pathology

Publishing model
Hybrid

Submit your manuscript

Kocaeli Üniversitesi | Explore open access funding | Change institution

Favorite Export

JCR Year 2024

VIRCHOWS ARCHIV

ISSN

0945-6317

EISSN

1432-2307

JCR ABBREVIATION

VIRCHOWS ARCH

ISO ABBREVIATION

Virchows Arch.

Journal information

EDITION

Science Citation Index Expanded (SCIE)

CATEGORY

PATHOLOGY

LANGUAGES	REGION	1ST ELECTRONIC JCR YEAR
English	GERMANY (FED REP GER)	1997

Publisher information

PUBLISHER	ADDRESS	PUBLICATION FREQUENCY
SPRINGER	ONE NEW YORK PLAZA, SUITE 4600 , NEW YORK, NY 10004, UNITED STATES	12 issues/year

Journal's performance

Journal Impact Factor

The Journal Impact Factor (JIF) is a journal-level metric calculated from data indexed in the Web of Science Core Collection. It should be used with careful attention to the many factors that influence citation rates, such as the volume of publication and citations characteristics of the subject area and type of journal. The Journal Impact Factor can complement expert opinion and informed peer review. In the case of academic evaluation for tenure, it is inappropriate to use a journal-level metric as a proxy measure for individual researchers, institutions, or articles. Learn more

2024 JOURNAL IMPACT FACTOR	JOURNAL IMPACT FACTOR WITHOUT SELF CITATIONS
3.1	2.9
View calculation	View calculation

Journal Impact Factor Trend 2024

Export

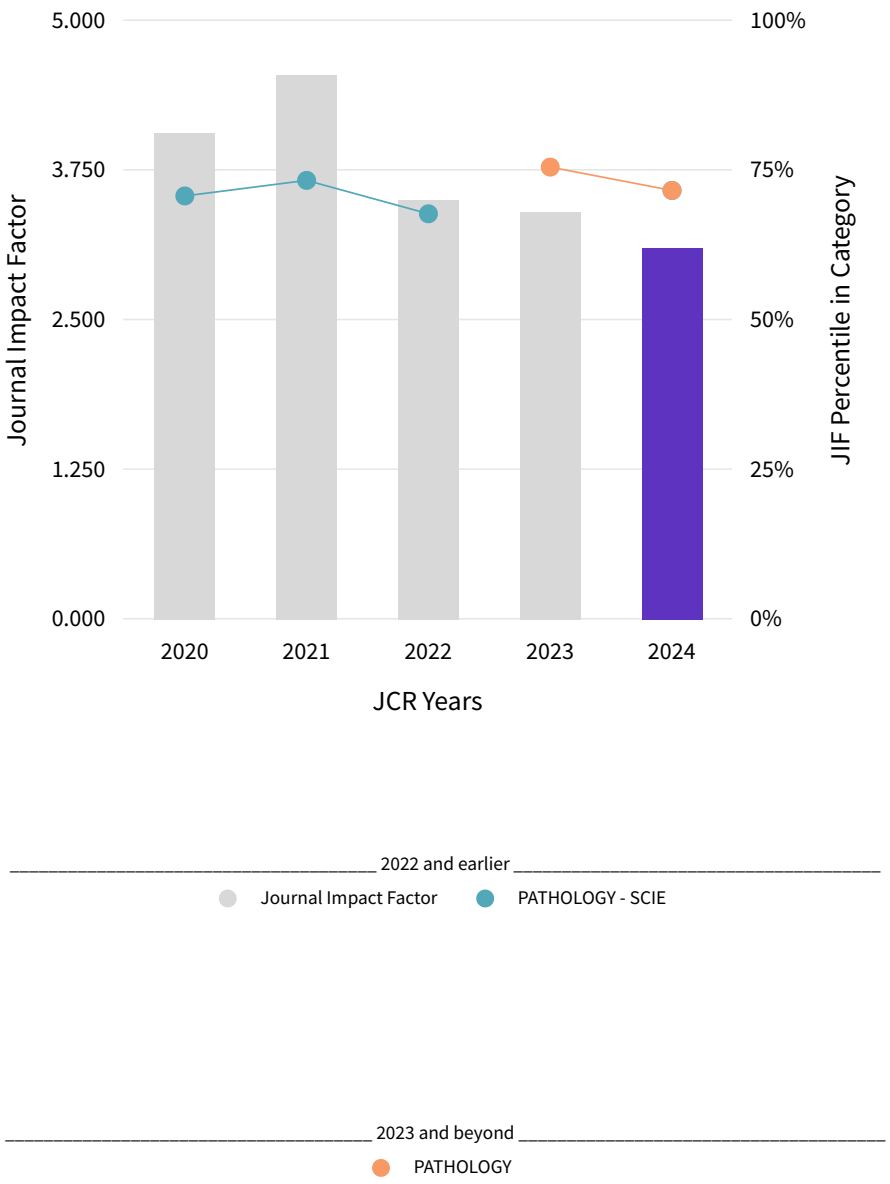
Journal Impact Factor contributing items

Export

Citable items (395) Citing Sources (491)

TITLE	CITATION COUNT
New concepts in EBV-associated B, T, and NK cell lymphoproliferative disorders	30
International Consensus Classification of acute lymphoblastic leukemia/lymphoma	27

15



View all years

The International Consensus Classification of acute myeloid leukemia	22
Standardized pathology report for HER2 testing in compliance with 2023…	21
Artificial intelligence-assisted cancer diagnosis improves the efficiency of…	20
Third International Consensus Conference on lesions of uncertain…	20
Updates on breast biomarkers	20
Plasma cell neoplasms and related entities-evolution in diagnosis and…	17
Comparison of HercepTest™ mAb pharmDx (Dako Omnis, GE001) with…	15
Diagnostic approaches and future directions in Burkitt lymphoma and hig…	14

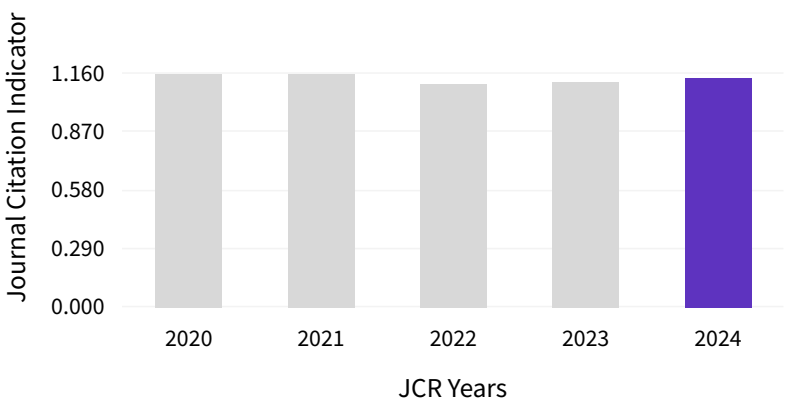
View All in Web of Science

Journal Citation Indicator (JCI)

Export

1.14

The Journal Citation Indicator (JCI) is the average Category Normalized Citation Impact (CNCI) of citable items (articles & reviews) published by a journal over a recent three year period. The average JCI in a category is 1. Journals with a JCI of 1.5 have 50% more citation impact than the average in that category. It may be used alongside other metrics to help you evaluate journals. Learn more



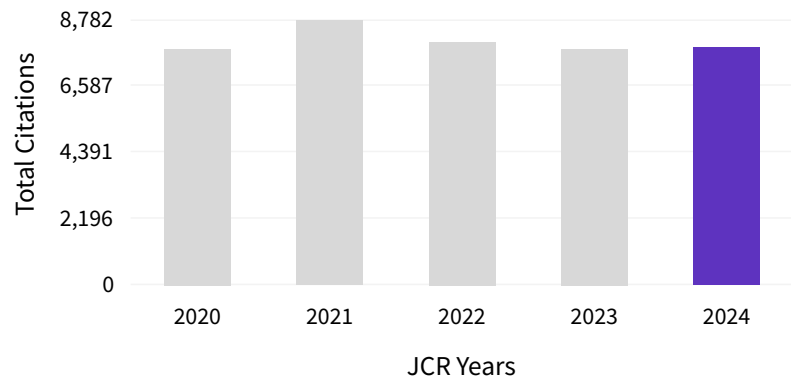
View all years

Total Citations

Export

7,888

The total number of times that a journal has been cited by all journals included in the database in the JCR year. Citations to journals listed in JCR are compiled annually from the JCR years combined database, regardless of which JCR edition lists the journal.



View all years

15

Citation distribution

Export

The Citation Distribution shows the frequency with which items published in the year or two years prior were cited in the JCR data year (i.e., the component of the calculation of the JIF). The graph has similar functionality as the JIF Trend graph, including hover-over data descriptions for each data point, and an interactive legend where each data element's legend can be used as a toggle. You can view Articles, Reviews, or Non-Citable (other) items to the JIF numerator. Learn more

ARTICLE CITATION MEDIAN

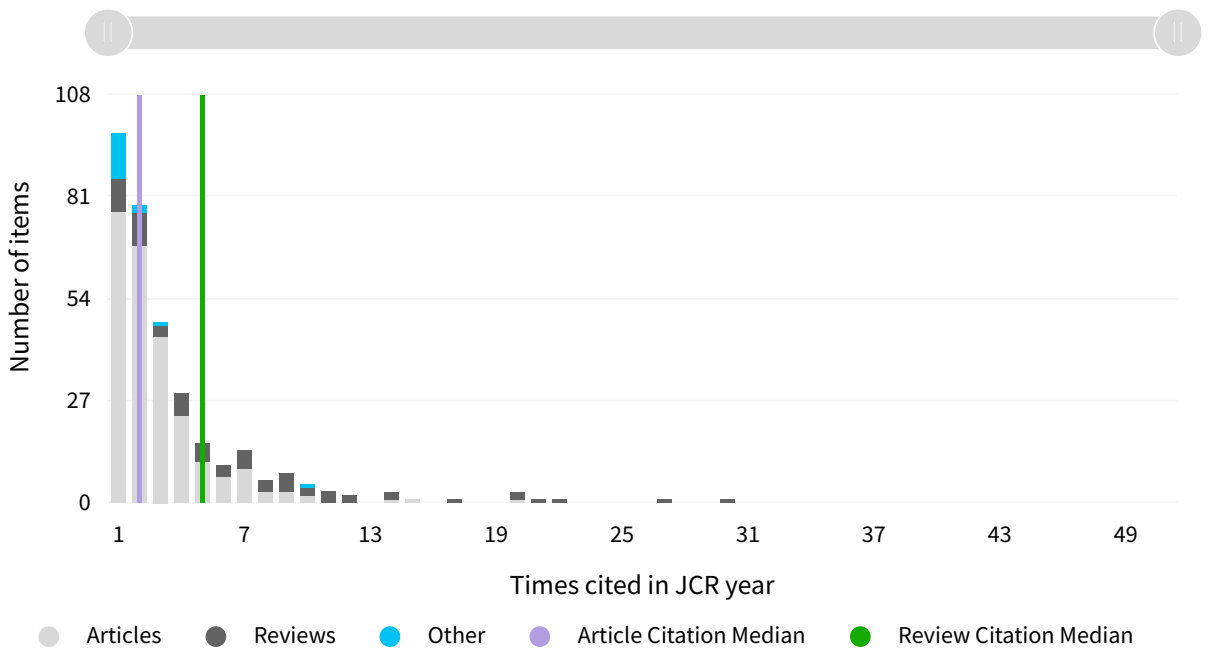
2

REVIEW CITATION MEDIAN

5

UNLINKED CITATIONS

16



TIMES CITED

0

ARTICLES

73

REVIEWS

8

OTHER

1,226

Open Access (OA)

Export

The data included in this tile summarizes the items published in the journal in the JCR data year and in the previous two years. This three-year set of published items is used to provide descriptive analysis of the content and community of the journal. Learn more

Items

TOTAL CITABLE	% OF CITABLE OA
640	40.63%

Citations*

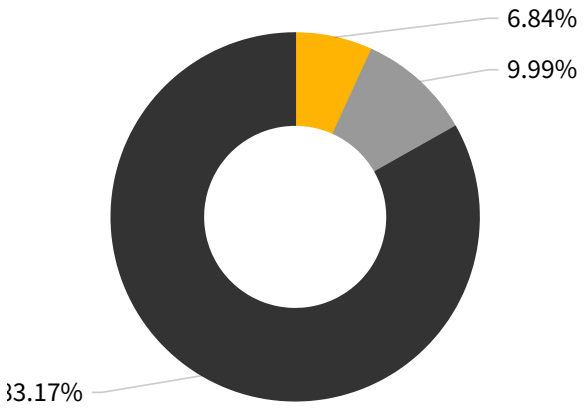
TOTAL CITABLE	% OF CITABLE OA
1,328	53.46%

15

CITABLE

GOLD OPEN ACCESS
260 / 6.84%

SUBSCRIPTION AND FREE TO READ
380 / 9.99%



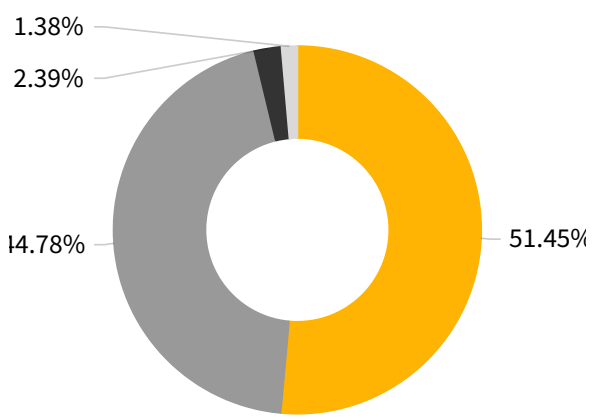
NON-CITABLE

OTHER (NON CITABLE ITEMS)
3,162 / 83.17%

CITABLE

GOLD OPEN ACCESS
710 / 51.45%

SUBSCRIPTION AND FREE TO READ
618 / 44.78%



NON-CITABLE

OTHER (NON CITABLE ITEMS)
33 / 2.39%

UNLINKED CITATIONS
19 / 1.38%

*Citations in 2024 to items published in [2022 - 2024]

Rank by Journal Impact Factor

Journals within a category are sorted in descending order by Journal Impact Factor (JIF) resulting in the Category Ranking below. A separate rank is shown for each category in which the journal is listed in JCR. Beginning in 2023, ranks are calculated by category.
Learn more

CATEGORY
PATHOLOGY

26/90

JCR YEAR	JIF RANK	JIF QUARTILE	JIF PERCENTILE
2024	26/90	Q2	71.7
2023	22/88	Q1	75.6

Rank by JIF before 2023 for PATHOLOGY

EDITION
Science Citation Index Expanded (SCIE)

JCR YEAR	JIF RANK	JIF QUARTILE	JIF PERCENTILE
2022	25/76	Q2	67.8
2021	21/77	Q2	73.38
2020	23/77	Q2	70.78
2019	24/78	Q2	69.87

Rank by Journal Citation Indicator (JCI)

15

Journals within a category are sorted in descending order by Journal Citation Indicator (JCI) resulting in the Category Ranking below. A separate rank is shown for each category in which the journal is listed in JCR. Data for the most recent year is presented at the top of the list, with other years shown in reverse chronological order. Learn more

CATEGORY

PATHOLOGY

19/90

JCR YEAR	JCI RANK	JCI QUARTILE	JCI PERCENTILE
2024	19/90	Q1	79.44
2023	17/88	Q1	81.25
2022	24/87	Q2	72.99
2021	20/89	Q1	78.09
2020	19/90	Q1	79.44
2019	22/89	Q1	75.84
2018	21/89	Q1	76.97

Citation network

Cited Half-life

6.7 years

The Cited Half-Life is the median age of the items in this journal that were cited in the JCR year. Half of a journal's cited items were published more recently than the cited half-life.

TOTAL NUMBER OF CITES

7,888

NON SELF-CITATIONS

7,623

SELF-CITATIONS

265

Citing Half-life

6.4 years

The Citing Half-Life is the median age of items in other publications cited by this journal in the JCR year.

TOTAL NUMBER OF CITES

8,453

NON SELF-CITATIONS

8,188

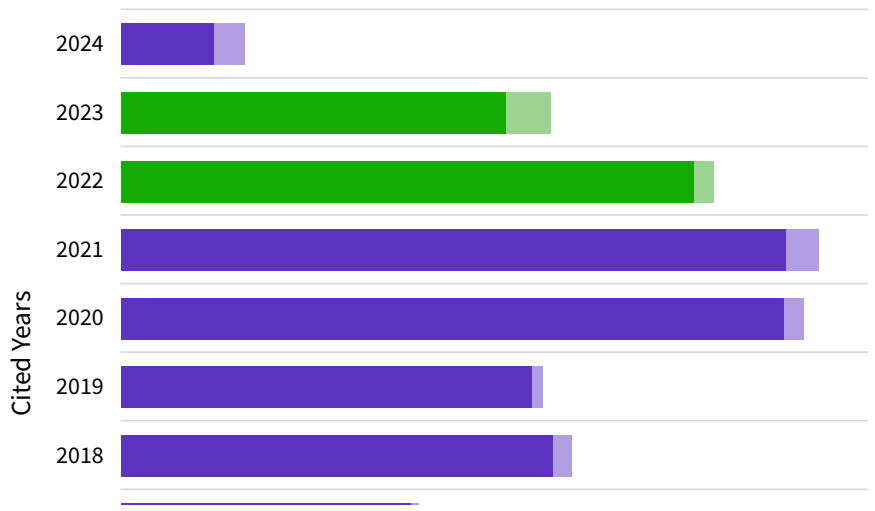
SELF-CITATIONS

265

Cited Half-life Data | Citing Half-life Data

Export

15

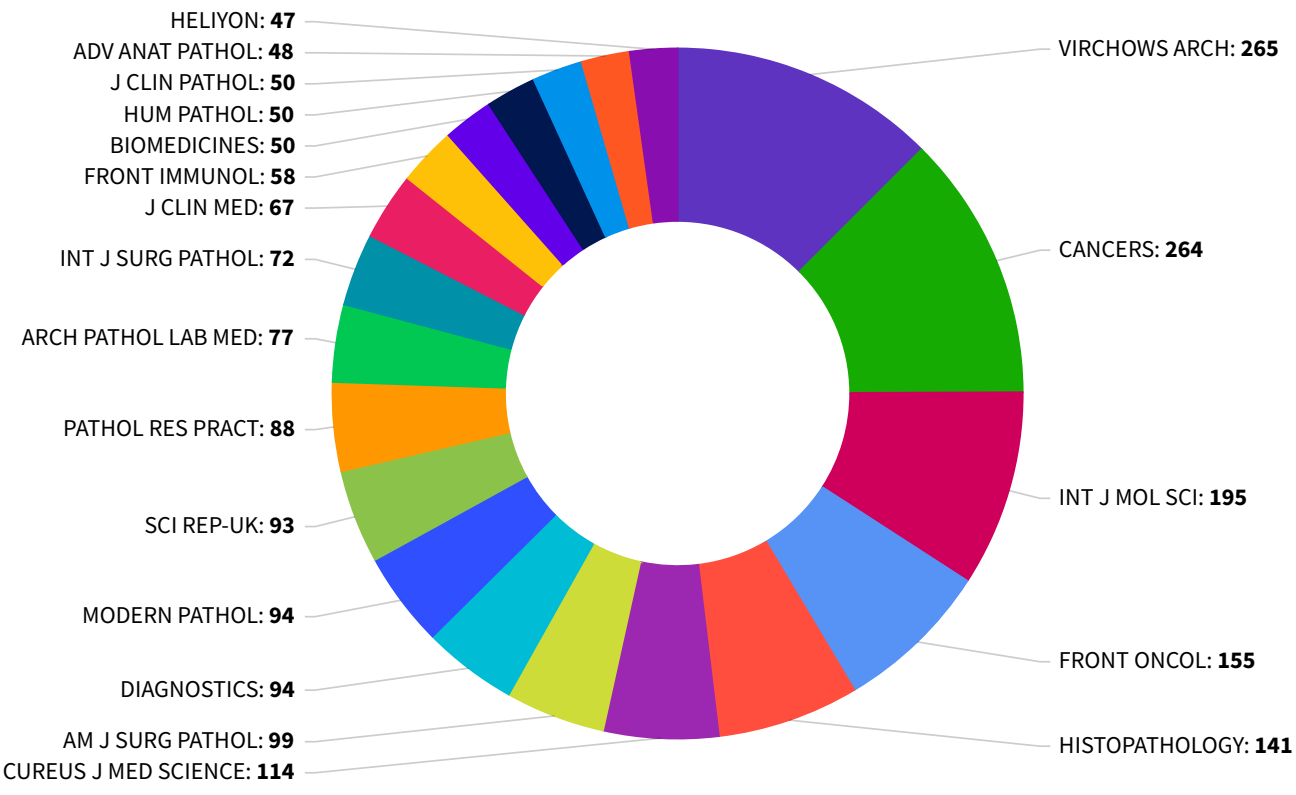


CITED YEAR	# OF CITES FROM 2024	CUMULATIVE %	# OF CITING SOURCES
All years	**7,888 citations**	**100.00%**	**1,801 sources**
2024	149 citations	1.89%	71 sources
2023	517 citations	8.44%	244 sources
2022	714 citations	17.49%	356 sources
2021	839 citations	28.13%	419 sources
2020	822 citations	38.55%	412 sources
2019	507 citations	44.98%	318 sources
2018	542 citations	51.85%	314 sources

Journal Citation Relationships

Cited Data | Citing Data

Top 20 journals citing VIRCHOWS ARCH by number of citations



Content metrics

Source data

This tile shows the breakdown of document types published by the journal. Citable Items are Articles and Reviews. For the purposes of calculating JIF, a JCR year considers the publications of that journal in the two prior years. Learn more

Average JIF Percentile

Export

The Average Journal Impact Factor Percentile takes the sum of the JIF Percentile rank for each category under consideration then calculates the average of those values. Learn more

15

245 total citable items

	ARTICLES	REVIEWS	COMBINED(C)	OTHER DOCUMENT TYPES(O)	PERCENTAG
NUMBER IN JCR YEAR 2024 (A)	215	30	245	1,920	11%
NUMBER OF REFERENCES (B)	6,272	2,071	8,343	110	99%
RATIO (B/A)	29.2	69.0	34.1	0.1	

ALL CATEGORIES AVERAGE
71.7

PATHOLOGY
71.7

Contributions by organizations

Export

Organizations that have contributed the most papers to the journal in the most recent three-year period. Learn more

RANK	ORGANIZATION	COUNT
1	UNIVERSITE DE TUNIS-EL-MANAR	100
2	CHARLES UNIVERSITY PRAGUE	73
3	UNIVERSITY OF ERLANGEN NUREMBERG	55
4	UNIVERSIDADE DE COIMBRA	52
5	UNIVERSITY OF BARCELONA	47
6	UNIVERSITE DE SFAX	43

Contributions by country/region

Export

Countries or Regions that have contributed the most papers to the journal in the most recent three-year period. Learn more

RANK	COUNTRY / REGION	COUNT
1	SPAIN	413
2	ITALY	340
3	USA	301
4	TURKIYE	252
5	PORTUGAL	246
6	TUNISIA	239
7	GERMANY (FED REP GER)	225
8	ROMANIA	168
9	RUSSIA	153

Additional metrics

Eigenfactor Score

0.00833

The Eigenfactor Score is a reflection of the density of the network of citations around the journal using 5 years of cited content as cited by the Current Year. It considers both the number of citations and the source of those citations, so that highly cited sources will influence the network more than

Normalized Eigenfactor

1.86673

The Normalized Eigenfactor Score is the Eigenfactor score normalized, by rescaling the total number of journals in the JCR each year, so that the average journal has a score of 1. Journals can then be compared and influence measured by their score relative to 1. Learn more

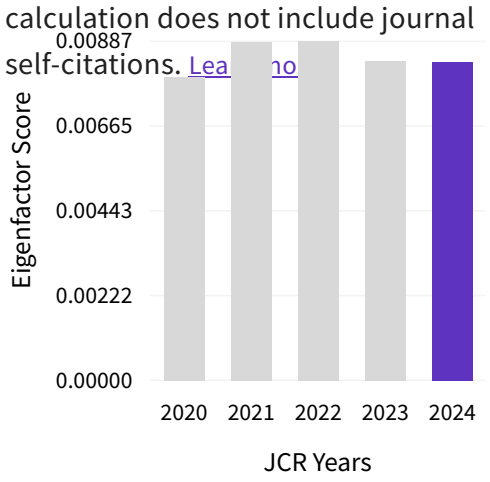
Article influence score

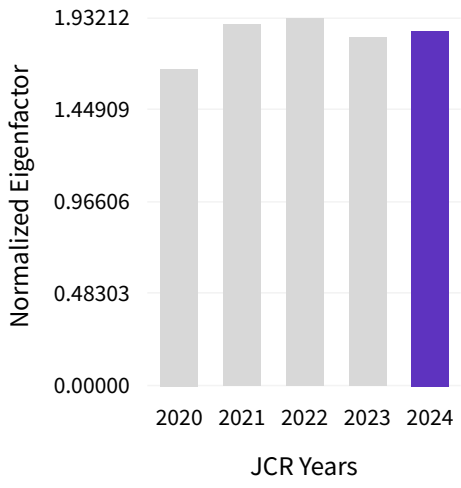
1.010

The Article Influence Score normalizes the Eigenfactor Score according to the cumulative size of the cited journal across the prior five years. The mean Article Influence Score for each article is 1.00. A score greater than 1.00

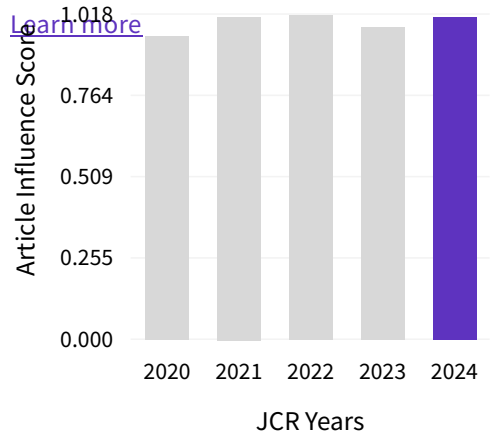
15

less cited sources. The Eigenfactor calculation does not include journal self-citations. Lea[illegible]no





indicates that each article in the journal has above-average influence. Learn more

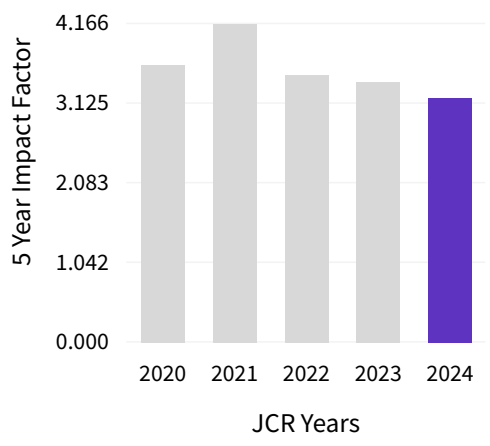


5 Year Impact Factor

3.2

View Calculation

The 5-year Impact Factor is the average number of times articles from the journal published in the past five years have been cited in the JCR year. It is calculated by dividing the number of citations in the JCR year by the total number of articles published in the five previous years. Learn more

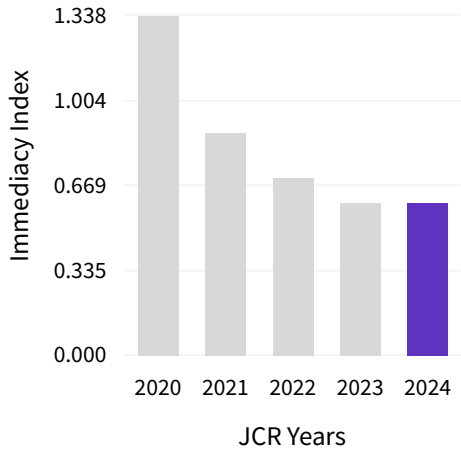


Immediacy Index

0.6

View Calculation

The Immediacy Index is the count of citations in the current year to the journal that reference content in this same year. Journals that have a consistently high Immediacy Index attract citations rapidly. Learn more



© 2025 Clarivate

Legal center

Privacy notice

Cookie policy

Terms of Use

Manage cookie preferences

Copyright notice

Accessibility

Help

SPRINGER NATURE Link

Log in

Menu Search Cart

Home › Virchows Archiv › Editorial board



Virchows Archiv

Publishing model: **Hybrid**

Kocaeli Üniversitesi Explore open access funding | Change institution

Journal menu

Editorial board

Editor-in-Chief

Abbas Agaimy, MD, *University of Erlangen, Germany*

Senior Editorial Consultant

Sigurd F. Lax, MD, PhD, *Hospital of the Medical University of Graz, Linz, Austria*

Review Editor

Leticia Quintanilla-Martinez, MD, *University of Tübingen, Germany*

Associate Editors

Irene Esposito, MD, *University of Düsseldorf, Germany*

Yoshinao Oda, MD, PhD, *Kyushu University, Fukuoka, Japan*

Leticia Quintanilla-Martinez, MD, PhD, *University of Tübingen, Germany*

Kiril Trpkov, MD, PhD, *University of Calgary, Alberta, Canada*

Editorial Board

Rita Alaggio, MD, *University of Padua, Rome, Italy*

Alyaa Al-Ibraheemi, MD, *Harvard Medical School, Boston, MA, USA*

Kerstin Amann, MD, PhD, *University of Erlangen, Germany*

Cristina R. Antonescu, MD, *Memorial Sloan Kettering Cancer Centre, New York, NY, USA*

Judith Bovée, MD, PhD, *Leiden University Medical Center, Leiden, The Netherlands*

Kyle Bradley, MD, MS, *Emory University, Atlanta, GA, USA*

Thomas Brenn, MD, PhD, *University of Michigan, Ann Arbor, MI, USA*

Reinhard Büttner, MD, *University of Bonn, Germany*

Jamie Eduardo Calonje, MD, *St Thomas' Hospital, London, UK*

Liang Cheng, MD, *Brown University, Providence, RI, USA*

Beatrix Cochand-Priollet, MD, PhD, *University Paris-Cité, Paris, France*

Ben Davidson, MD, PhD, *Oslo University Hospital, Oslo, Norway*

Angelo P. Dei Tos, MD, *University of Padua, Italy*

Ronald de Krijger, MD, PhD, *Erasmus University Rotterdam, The Netherlands*

Laurence de Leval, MD, PhD, *Lausanne University Hospital, Lausanne, Switzerland*

Michael den Bakker, MD, PhD, *Erasmus University Rotterdam, The Netherlands*

Josephine K. Dermawan, MD, PhD, *Cleveland Clinic, Cleveland, OH, USA*

Brendan C. Dickson, MD, *Sinai Health, Toronto, Canada*

Joachim Diebold, MD, PhD, *Lucerne Cantonal Hospital, Lucerne, Switzerland*

Catarina Eloy, MD, PhD, *University of Porto, Portugal*

Arzu Ensari, MD, PhD, *Ankara University Medical School, Ankara, Turkey*

Fabio Facchetti, MD, PhD, *University of Brescia, Italy*

Roger Feakins, MD, *University College London, UK*

Falko Fend, MD, PhD, *Tübingen University Hospital, Tübingen, Germany*

Andrew L. Folpe, MD, *Mayo Clinic College of Medicine, Rochester, MN, USA*

Maria Pia Foschini, MD, *University of Bologna, Italy*

Alessandro Franchi, MD, *University of Pisa, Italy*

John Gross, MD, PhD, *Johns Hopkins University School of Medicine, Baltimore, MA, USA*

John Hanna, MD, PhD, *Harvard Medical School, Boston, MA, USA*

C Simon Herrington, MD, PhD, *The University of Edinburgh, Scotland, UK*

Jason L. Hornick, MD, PhD, *Harvard Medical School, Boston, MA, USA*

Pei Hui, MD, PhD, *Yale University, New Haven, CT, USA*

Yin P. Hung, MD, PhD, *Massachusetts General Hospital, Harvard Medical School, Boston, MA, USA*

Deepali Jain, MD, *All India Institute of Medical Sciences, New Delhi, India*

Janina Kulka, MD, PhD, *Semmelweis University, Budapest, Hungary*

Stefano La Rosa, MD, *University of Insubria, Varese, Italy*

Gregory Y. Lauwers, MD, *Moffitt Cancer Center, Tampa, FL, USA*

Alexander Lazar, MD, PhD, *MD Anderson Cancer Centre, Houston, TX, USA*

Antonio Lopez-Beltran, MD, PhD, *University of Cordoba, Spain*

Claudio Luchini, MD, PhD, *University of Verona, Italy*

Isidro Machado, MD, PhD, *Instituto Valenciano de Oncología, Valencia, Spain*

Xavier Matias-Guiu, MD, PhD, *The University Hospital Arnau de Vilanova, Barcelona, Spain*

W Glenn McCluggage, MD, *Royal Victoria Hospital, Belfast, UK*

Thomas Mentzel, MD, *Reference Center for Dermatopathology, Friedrichshafen, Germany*

Michael Michal, MD, PhD, *Charles University, Pilsen, Czech Republic*

Markku Miettinen, MD, PhD, *National Cancer Institute, Bethesda, MD, USA*

Holger Moch, MD, PhD, *University Hospital of Zürich, Switzerland*

Rodolfo Montironi, MD, *Marche Polytechnic University, Ancona, Italy*

Vania Nosé, MD, PhD, *Harvard Medical School, Boston, MA, USA*

David J. Papke Jr., MD, PhD, *Harvard Medical School, Boston, MA, USA*

Mauro Papotti, MD, *University of Turin, Italy*

Aurel Perren, MD, PhD, *University of Bern, Switzerland*

Bharat Rekhi, MD, *Tata Memorial Hosptial, Mumbai, India*

Guido Rindi, MD, PhD, *Catholic University of the Sacred Heart, Rome, Italy*

Christoph Röcken, MD, PhD, *University Hospital Schleswig Holstein, Kiel, Germany*

Lisa Rooper, MD, *Johns Hopkins Hospital, Baltimore, MD, USA*

Andreas Rosenwald, MD, *University of Würzburg, Germany*

Esther Diana Rossi, MD, PhD, *Policlinico Universitario Fondazione Agostino Gemelli, Rome, Italy*

Anna Sapino, MD, PhD, *University of Turin, Italy*
Aldo Scarpa, MD, PhD, *University of Verona, Italy*
Inga-Marie Schaefer, MD, *Harvard Medical School, Boston, MA, USA*
Peter Schirmacher, MD, PhD, *University Hospital Heidelberg, Germany*
Fernando Schmitt, MD, PhD, *University of Porto, Portugal*
Alena Skálová, MD, PhD, *Biopticka Laboratory, Pilsen, Czech Republic*
David I. Suster, MD, *Massachusetts General Hospital, Newark, NJ, USA*
Puay-Hoon Tan, MD, *Singapore General Hospital, Singapore*
Khin Thway, MD, *The Royal Marsden, London, UK*
Tibor Tot, MD, PhD, *University of Uppsala, Falun, Sweden*
Toyonori Tsuzuki, MD, PhD, *Aichi Medical University, Nagakute, Japan*
Marc van de Vijver, MD, PhD, *Amsterdam University Medical Center, Amsterdam, The Netherlands*
Zsuzsanna Varga, MD, PhD, *University Hospital Zurich, Switzerland*
Giuseppe Viale, MD, *European Institute of Oncology, Milan, Italy*
Ilan Weinreb, MD, PhD, *University of Toronto, ON, Canada*
Wentao Yang, MD, PhD, *Fudan University, Shanghai, China*
Akihiko Yoshida, MD, PhD, *National Cancer Center Research Institute, Tokyo, Japan*
Giuseppe Zamboni, MD, PhD, *University of Verona, Italy*
Nina Zidar, MD, PhD, *University of Ljubljana, Slovenia*

President, Secretary and Treasurer of ESP

Prof Xavier Matais-Guiu, *Universitat de Lleida, Lleida, Spain*
Prof Metka Volavšek, *University of Ljubljana, Ljubljana, Slovenia*
Prof Maria Rosaria Raspollini, *University Hospital Careggi, Florence, Italy*

Past Editors

Daniela Massi, *Florence, Italy*
N. Volkan Adsay, *Atlanta, GA, USA*
Fred T. Bosman, *Lausanne, Switzerland*
Maria de Fátima Carneiro, *Porto, Portugal*
Manfred Dietel, *Berlin, Germany*

Vincenzo Eusebi, *Bologna, Italy*

Masashi Fukayama, *Tokyo, Japan*

Heinz Höfler, *Munich, Germany*

Günter Klöppel, *Munich, Germany*

Hans Kreipe, *Hannover, Germany*

Han van Krieken, *Nijmegen, The Netherlands*

Sunil Lakhani, *Brisbane, Australia*

Cord Langner, *Graz, Austria*

George Netto, *Birmingham, AL, USA*

Ales Ryska, *Hradec Kralove, Czech Republic*

Manuel Sobrinho-Simões, *Porto, Portugal*

Laura J. Tafe, *Lebanon, NH, USA*

Virchows Archiv
https://doi.org/10.1007/s00428-025-04264-6

ORIGINAL ARTICLE

Solitary fibrous tumor of kidney and renal hilus: a multi-institutional clinicopathologic analysis of 43 cases

Güneş Güner[1] · Mahmut Akgul[2] · Michael Michal[3,4] · Asli Yilmaz[5] · Buşra Yaprak Bayrak[6] · Bermal Hasbay[7] · Aylin Yazgan[8] · Nilüfer Kandemir[8] · Murat Oktay[9] · Deniz Bayçelebi[10] · Arkar Htoo[11] · Jose Lopez[12] · Ondrej Hes[4] · Arndt Hartmann[15] · Dilek E. Baydar[13] · Kril Trpkov[5] · Sambit K. Mohanty[14] · Abbas Agaimy[15] · Pedram Argani[16] · Kemal Kösemehmetoğlu[1]

Received: 26 August 2025 / Revised: 26 August 2025 / Accepted: 31 August 2025
© The Author(s), under exclusive licence to Springer-Verlag GmbH Germany, part of Springer Nature 2025

Abstract

Solitary fibrous tumor (SFT) is a fibroblastic neoplasm characterized by prominent, staghorn, or delicate "hemangiopericytoma (HPC)-like vasculature", *NAB2::STAT6* gene fusion, and its surrogate STAT6 expression. SFT may exhibit an unpredictable clinical course, necessitating risk assessment based on tumor characteristics. Renal SFTs are rare and have not been well characterized. Forty-three primary kidney SFT cases are reviewed for clinical, morphological, and immunohistochemical (STAT6, BCL2, CD34, and PAX8) features. A four-variable risk stratification by Demicco was applied based on patient age, tumor size, mitotic activity, and tumor necrosis. The mean age was 49 years (range 11–83 years) with a slight female predominance (male:female = 20:23). The mean tumor size was 7.8 cm (1.6–32 cm). Tumors were mainly located at the hilus (22/32, 68%) and had well-demarcated borders (31/42, 74%). Morphologically, tumors were categorized as 1) Fibrous ("SFT-like", 19/43, 44%), characterized by hypocellularity and prominent fine-reticular or keloidal collagen; 2) Cellular ("HPC-like", 8/43, 19%), with hypercellularity, short spindle to small cell-like proliferation, and lacking a collagenous background; 3) mixed fibrous/cellular (16/43, 37%) displaying both components. Four cases featured a lipomatous component. BCL2 was positive in all tested cases (28/28), CD34 in all but 3 cases (93%), and STAT6 in all but one case (39/40, 97.5%). PAX8 was positive in 6/34 (18%) cases. Most cases (29/43, 68%) were classified as low-risk, followed by intermediate (12/43, 27%) and high-risk (2/43, 5%) groups. Five of 29 (18%) patients had metastatic disease, and two patients with high-risk and one with intermediate-risk tumors died from the disease, while 25 patients with low- or intermediate-risk tumors were alive for an average of about 36 months. We emphasize the usefulness of the risk stratification system in predicting prognosis. PAX8 expression in a subset of renal SFT represents a potential diagnostic pitfall.

Keywords Solitary fibrous tumor · Hemangiopericytoma · Renal · Kidney · STAT6 · PAX8 · Prognosis · Stratification

Introduction

Solitary fibrous tumor is a mesenchymal neoplasm with fibroblastic differentiation and a characteristic *NAB2*::*STAT6* gene Fusion, presenting mostly in the 4th to 7th decades of life with equal sex distribution [1, 2]. Although originally reported in the pleura (hence the descriptive term SFT to distinguish it from diffuse mesotheliomas), SFT has been shown to occur at any body sites, albeit rare. These tumors are mostly well-delineated, solid lesions with variable amounts of collagen deposition and spindle cells, with fat-forming SFT as a rare subtype [3]. They can emerge from nearly all body sites, resulting in an extensive list of differential diagnoses [4, 5].

SFT of the kidney is relatively rare, with around 100 cases reported in the English literature [6–16]. It displays a variety of clinical features such as localization in the renal pelvis and urinary flow obstruction [4, 17], late distant metastases [18, 19], local recurrences [20], contralateral recurrence [9], bilateral kidney involvement [21], multiple lesions in the same kidney [22], cystic change [14], along with extremely rare presentations like originating from the wall of the renal vein [23], extending into the inferior vena cava and the right atrium [24], lymph node metastasis [25], and paraneoplastic hypoglycemia [22, 26]. SFT arising from the kidney and the retroperitoneum can manifest with signs

Extended author information available on the last page of the article

and symptoms resembling renal cell carcinoma [16], and these two can co-exist [27]. This variability in presentation underlines the importance of histopathological assessment in both the diagnosis and prognostication of this tumor.

In the appropriate morphological context, positive STAT6 expression by immunohistochemistry (IHC) is considered a diagnostic gold standard of SFT. However, renal SFT is reported to express PAX8 [10, 28], EMA [7, 29], BCOR [30], or manifest with *NF1* mutation in addition to its signature *NAB2*::*STAT6* alteration [31]. This report presents 43 cases of renal SFT, with an emphasis on pertinent histological features and an attempt to classify them morphologically. Moreover, risk assessment was performed using the four-variable risk score outlined by Demicco et al. [32].

Material and methods

Sixteen institutions contributed a total of 43 renal SFT cases. For 16 cases, IHC was performed using a Leica Bond Max 2 Autostainer for STAT6 (11 cases: BioSB, EP325, 1/250 and 5 cases: Santa Cruz, D-1, 1:800), CD34 (Leica, QBEND-10, 1/100), BCL2 (Invitrogen, BCL-2–100-D5, 1/600), and PAX8 (11 cases: CellMarque, MRQ-50, 1/150 and 5 cases: Proteintech, 10336–1-AP, 1:800). For the remaining cases identified in the authors' consultation files, IHC was performed in different laboratories, with staining variations from case to case based on tissue availability and the initial differential diagnostic considerations on a case-by-case basis (details of the staining protocols and antibody sources are available upon request). Biomarker expression was scored as diffuse (> 50% of positive expression in tumor cells), focal (< 50% of positive expression in tumor cells), or negative (no expression).

Follow-up data were collected from the institutions' computer-based patient databases. Parameters described by Demicco et al. [32] were used to segregate cases into low, intermediate, or high-risk groups, as summarized in Table 1. This risk stratification was designed using primary non-meningeal SFTs; the cohort had a 7% risk of 10-year metastasis in intermediate-risk cases and a 49% rate of 5-year metastasis in high-risk cases.

Table 1 Demicco's risk stratification system for solitary fibrous tumor

	Risk factor	Score
Age	< 55	0
	≥ 55	1
Tumor size (cm)	< 5	0
	5 to < 10	1
	10 to < 15	2
	≥ 15	3
Mitotic count (/10 high-power fields)	0	0
	1–3	1
	≥ 4	2
Tumor necrosis	< 10%	0
	≥ 10%	1
Risk classification	*Total score*	
Low	0–3	
Intermediate	4–5	
High	6–7	

This stratification is taken from Demicco et al. PMID: 28731041

Results

The clinical, morphological, and IHC features of the cases are summarized in Table 2 and Fig. 1. The mean age was 49 (range: 11–83), with a slight female predilection (1:1.15). The mean tumor size was 7.8 cm (range: 1.6—32). The right and left kidneys were nearly equally involved. Masses were mostly located in the hilus or peripelvic fat (22 cases, 69%), but intrarenal tumors were also present (10 cases, 31%); tumor location was not available for 11 cases (Fig. 2). Tumors were primarily well-circumscribed, multinodular, and had a tan to white cut surface (Fig. 3). All cases diagnosed with either partial or radical nephrectomy, except for a patient diagnosed with a core biopsy (Case #37). A patient (#13) who underwent marginal excision and was diagnosed with SFT and surgical margin positivity was suspected of recurrence after 1.5 years; however, radical nephrectomy of the remaining non-functional kidney revealed no residual tumor or recurrence.

Three different morphologies were present: 1) the fibrous or "classical SFT" pattern ("SFT-like") with a collagenous background (usually with keloidal collagen), hypocellularity, and inflammation (19 cases, 44%, Fig. 4a-b); 2) the cellular or "so-called hemangiopericytoma" pattern ("HPC-like") with a storiform configuration, delicate vessels, intermediate to high cellularity, short spindle to small round cells, and no or minimal collagen (8 cases, 19%, Fig. 4c-d); and 3) the mixed pattern that combines these two morphologies (16 cases, 37%, Fig. 4e-f). Two cases with mixed patterns and two with fibrous patterns also exhibited lipomatous areas consistent with lipomatous SFT. Tumors were well-demarcated in most cases (74%), with 11 (26%) showing infiltrative borders. Only one intermediate-risk (Case #30) and one high-risk tumor (Case #42) exhibited frank invasion of surrounding tissues, and the patient with high-risk HPC-like morphology died from the disease six months after diagnosis. Accompanying morphological features included myxoid change (15 cases, 35%, Fig. 5a), bone metaplasia (1 case, Fig. 5b), lipoblast-like cells (1 case, Fig. 5c), renal tubular entrapment (3 cases, Fig. 5d), necrosis (9 cases,

Table 2 Features of renal solitary fibrous tumor cases

#	Age (yrs)	Sex	Size (cm)	Location	Borders	Fibrous/ Cellular	Necrosis	Mitosis (10 HPF)	CD34	BCL2	STAT6	PAX8	Risk score*	Follow-up	Other
1	53	M	2.5	Hilus	WD	Fibrous	-	0	+	NA	-	-	0-Low	NED, 48 mos	Keloidal collagen, myxoid degeneration, accompanying infl
2	42	F	2.6	R, mid	WD	Fibrous Lipomatous	-	0	+	+	+	-	0-Low	NED, 1 mo	Keloidal collagen, hyalinized large vessels, entrapped renal tubules, fat-forming
3	47	F	4.3	NA	WD	Mixed	-	0	+	+	+	-	0-Low	NA	
4	44	F	3.8	R, lower hilus	min inf	Mixed	-	0	+	NA	+	NA	0-Low	NED, 1 mo No mets	Vascular herniation
5	60	F	9	R, hilus	WD	Fibrous	-	0	+	+	+	-	1-Low	NA	Hyalinized vessels, ossification, keloidal collagen, accompanying infl
6	45	F	3.8	L	min inf	Fibrous	-	1	+	+	+	-	1-Low	NA	Entrapped tubules
7	39	F	5.2	R, hilus	min inf	Mixed	-	0	+	NA	+	-	1-Low	NED, 156 mos	
8	57	M	2.5	L, upper pole	WD	Mixed	-	3	+	+	+	-	1-Low	AWD, 84 mos Periaortic and lung mets at dx	
9	65	F	3	NA	WD	Cellular	-	0	F+	NA	+	+	1-Low	NED, 1 mo	Accompanying infl
10	30	M	3.7	L, lower pole	WD	Fibrous	-	1	+	+	+	-	1-Low	NED, 23 mos	Keloidal collagen
11	40	F	7.2	L, hilus	WD	Fibrous	-	0	+	+	+	-	1-Low	NED, 20 mos	Keloidal collagen
12	33	F	9	L, upper pole	WD	Fibrous	-	0	F+	NA	+	-	1-Low	NA	Storiform pattern

Table 2 (continued)

#	Age (yrs)	Sex	Size (cm)	Location	Borders	Fibrous/ Cellular	Necrosis	Mitosis (10 HPF)	CD34	BCL2	STAT6	PAX8	Risk score*	Follow-up	Other
13	58	M	5	R, hilus	WD	Fibrous	-	0	+	+	+	-	2-Low	NED, 24 mos	Keloidal collagen, accompanying infl
14	54	M	7	NA	min inf	Mixed Lipomatous	-	1	+	+	+	+	2-Low	NED, 7 mos	Myxoid degeneration, nodules with various differentiation, fat-forming
15	37	M	5	Hilus	min inf	Cellular	-	3	+	+	+	+	2-Low	NA	Accompanying infl
16	46	F	5.5	R, upper hilus	WD	Fibrous	-	3	+	+	+	NA	2-Low	NED, 12 mos	Accompanying infl., keloidal collagen, myxoid degeneration
17	24	M	7.6	R, lower hilus	min inf	Fibrous	-	1	+	+	NA	-	2-Low	NED, 62 mos	Accompanying infl., keloidal collagen
18	39	F	3	R, hilus	WD	Mixed	-	4	+	NA	+	-	2-Low	NED, 24 mos	Keloidal collagen, myxoid degeneration
19	11	F	6.3	L, lower hilus	WD	Mixed	-	2	+	+	NA	+	2-Low	NA	Keloidal collagen, myxoid degeneration
20	17	F	3	R, mid hilus	WD	Mixed	-	4	-	+	+	-	2-Low	NA	Keloidal collagen
21	67	F	1.6	Hilus	WD	Cellular	-	3	+	NA	+	NA	2-Low	NA	
22	72	F	5	R, lower hilus	min inf	Fibrous	-	2	+	+	F+	-	3-Low	NA	Vascular herniation, large areas of hyalinization
23	17	F	12.5	L, upper hilus	WD	Fibrous	-	1	+	+	+	-	3-Low	NED, 108 mos	Accompanying infl
24	83	M	5	R, upper hilus	WD	Mixed Lipomatous	-	1	+	+	+	-	3-Low	NED, 12 mos	Surgical margins +, myxoid degeneration, accompanying infl., lipoblast-like cells
25	40	M	3	R	WD	Cellular	+	4	F+	NA	F+	+	3-Low	NED, 33 mos	Myxoid degeneration
26	66	M	9	R, lower hilus	WD	Mixed	-	1	+	+	+	NA	3-Low	NED, 5 mos	Keloidal collagen, myxoid degeneration
27	52	M	7.8	L, upper hilus	min inf	Mixed	-	7	+	NA	+	-	3-Low	NED, 48 mos	Keloidal collagen, myxoid degeneration

Table 2 (continued)

#	Age (yrs)	Sex	Size (cm)	Location	Borders	Fibrous/ Cellular	Necrosis	Mitosis (10 HPF)	CD34	BCL2	STAT6	PAX8	Risk score*	Follow-up	Other
28	76	M	3.8	NA	WD	Fibrous	-	6	+	+	NA	NA	3-Low	NED, 64 mos	Entrapped tubules
29	71	F	9	L, lower hilus	WD	Fibrous Lipomatous	-	3	+	+	+	NA	3-Low	AWD, 60 mos	Keloidal collagen, fat-forming
30	44	M	6.8	L, mid	Inf	Fibrous	+	20	+	+	+	F+	4-Int	NED, 4 mos	
31	44	M	18.5	R, lower pole	WD	Mixed	-	2	+	+	+	-	4-Int	NED, 11 mos	Keloidal collagen, myxoid degeneration
32	48	M	6.8	L, upper pole	WD	Mixed	+	10	-	+	+	-	4-Int	NA	Keloidal collagen, myxoid degeneration
33	27	F	13	L, lower pole	WD	Mixed	-	5	+	NA	+	-	4-Int	NA	Myxoid degeneration, nodules with various differentiation, hyalinization areas
34	50	F	5.3	NA	WD	Fibrous	+	50	+	+	+	-	4-Int	NA	
35	35	F	13.5	Hilus	WD	Cellular	-	5	-	NA	+	NA	4-Int	NA	
36	67	M	6	R, mid hilus	WD	Fibrous	+	2	+	+	+	-	4-Int	NED, 36 mos	
37	65	F	4.5	R, lower pole		Mixed	+	5	+	NA	+	-	4-Int	DOD, 18 mos, Lung, liver, and nodal mets	Myxoid degeneration, hyalinization areas
38	56	M	12	L, upper pole	WD	Mixed	-	1	+	+	+	NA	4-Int	AWD, 52 mos	Accompanying infl
39	72	F	12	L, lower hilus	WD	Fibrous	-	6	+	+	+	-	5-Int	NED, 2 mos	Keloidal collagen, nodules with various differentiation

Table 2 (continued)

#	Age (yrs)	Sex	Size (cm)	Location	Borders	Fibrous/Cellular	Necrosis	Mitosis (10 HPF)	CD34	BCL2	STAT6	PAX8	Risk score*	Follow-up	Other
40	57	M	10	L	WD	Cellular	+	7	+	NA	F+	-	5-Int	NA Met to bone and lungs at dx	Myxoid degeneration
41	40	F	26	NA	WD	Cellular	-	5	F+	NA	F+	-	5-Int	NA	Myxoid degeneration
42	36	M	32	L	Inf	Cellular	+	7	+	NA	+	-	6-High	DOD, 6 mos Liver and lung mets at dx;	
43	71	M	16	R	min inf	Fibrous	+	3	+	+	+	NA	6-High	DOD, 20 mos Liver, lung, nodal mets	Accompanying infl., keloidal collagen
	49 (11–83)	M:F = 20:23	7.9 1.6–32)	R:L = 17:16 Hilus: 22 (69%)	31 WD 9 min inf 2 inf 1 NA	19 Fibrous 16 Mixed 8 Cellular 4 Lipomatous	21%	4.2 (0–50)	93%	100%	98% (10% F)	18%	29 Low 12 Int 2 High	22 NED 3 AWD 3 DOD 15 NA	42% keloidal collagen 35% myxoid degeneration 26% accompanying inflammation

AWD Alive with disease, *DOD* Dead of disease, *dx* diagnosis, *F* focal, *HPF* high power field, *inf* infiltrative, *infl* inflammation, *int* intermediate, *L* Left, mets: metastases, *min inf* minimal infiltration, *NA* not available, *NED* no evidence of disease, *R* Right, *WD* Well-demarcated,

* Four-variable risk score proposed by Demicco et al. PMID: 28731041

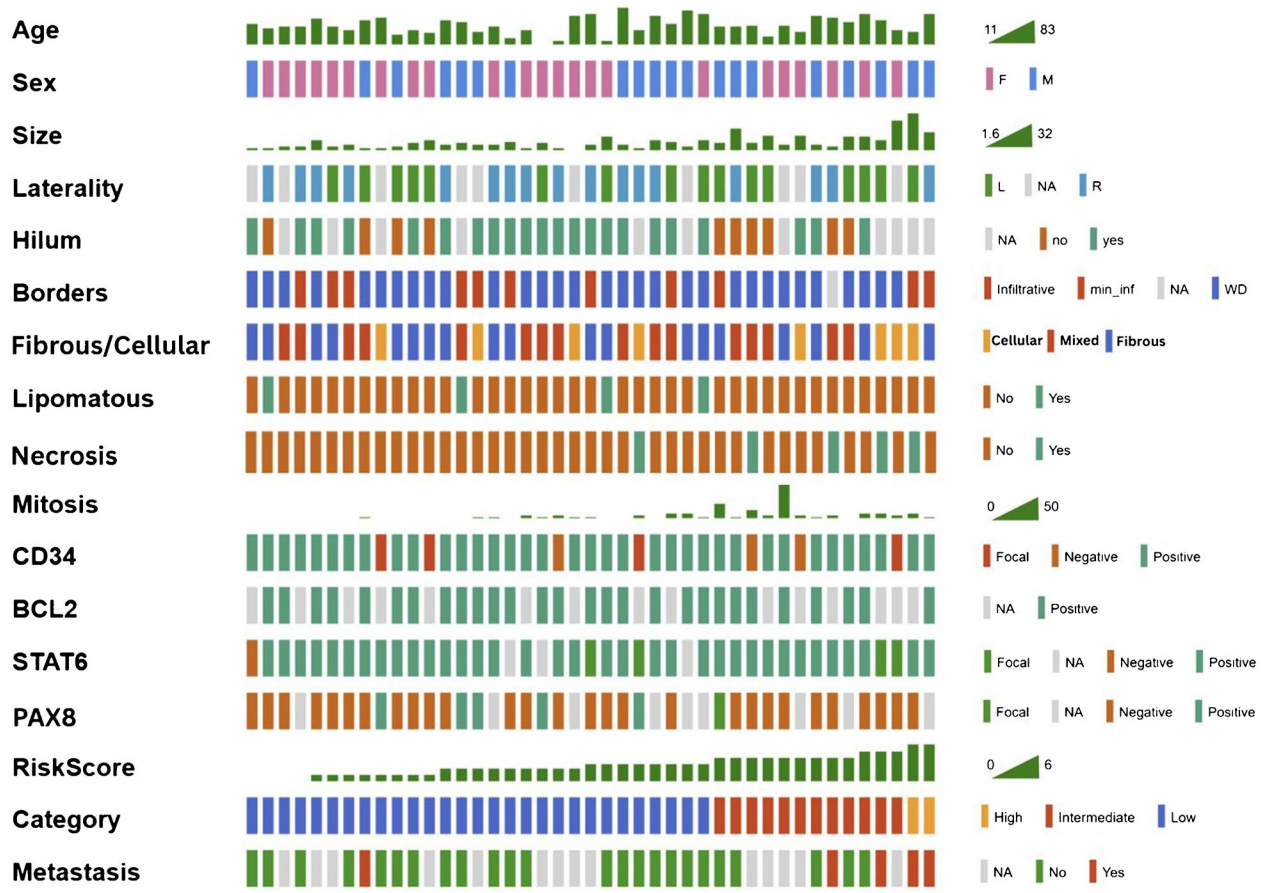


Fig. 1 Schematic illustration of the presented cases

21%, Fig. 5e), and vascular herniation in hilar veins (2 cases, Fig. 5f). Myxoid degeneration was commonly observed in the cellular pattern, whereas keloidal collagen was the hallmark of the fibrous pattern. Chronic inflammatory cells, primarily composed of lymphocytes and mast cells, were present in just over a quarter of the cases, regardless of morphological sub-classification.

All available cases ($n = 28$) were positive for BCL2, and 40/43 (93%) were positive for CD34. All but one case also expressed STAT6 (98%), with focal expression in 10% (Fig. 6). The case lacking STAT6 expression (case #1) exhibited a fibrous pattern and was diffusely positive for CD34 (Suppl. Figure 1). PAX8 was positive in 6/34 (18%) of the cases; all but one displayed either cellular or mixed patterns (Fig. 7). Significant findings regarding other immunostainings obtained from pathology reports included SMA (8 of 15 cases), CD99 (18 of 18 cases), and desmin (1/13) expressions, whereas pankeratin (12 cases), S100 (17 cases), and HMB45 (14 cases) were negative in all studied cases.

According to the Demicco stratification system, most tumors (29 cases, 67%) were classified as low-risk, followed by intermediate (12 cases, 28%) and high-risk (2 cases, 5%) groups. Among the 28 cases with follow-up data (mean follow-up period, 34 months; range, 1–156 months), 25 patients (89%) were alive with disease or with no evidence of disease for an average of 36 months; five patients (18%) had metastatic disease. Nineteen patients with low-risk SFT showed no evidence of disease for a mean of 40 months; one patient (Case #8) with a risk score of 3 (low-risk) presented with metastatic disease but has survived with the disease for 84 months (Suppl. Figure 2). The other four patients with metastasis had either intermediate (2) or high-risk (2) tumors. Two high- and one intermediate-risk patients died of disease at 6, 20, and 18 months, respectively.

Discussion

In this largest series in the literature, we presented the clinicopathological features of 43 SFTs of the kidney and renal hilus. Just over two-thirds of the tumors were located in the renal hilus, while about one-third of the cases undisputedly arose within the renal parenchyma; therefore, we refer to these cases as "SFT of kidney and renal hilus" or simply

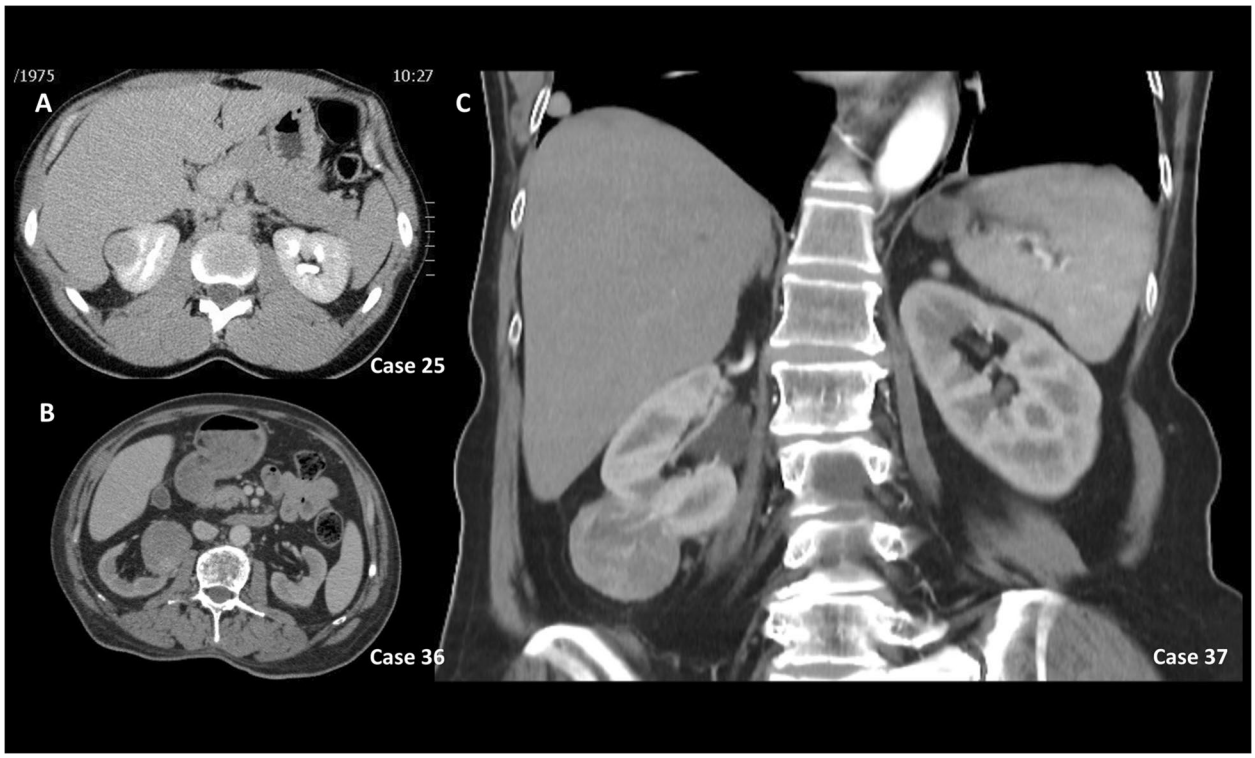


Fig. 2 Cross sections of computed tomography show exophytic intrarenal masses (**A** and **C**), while most tumors are in the renal hilus (**B**)

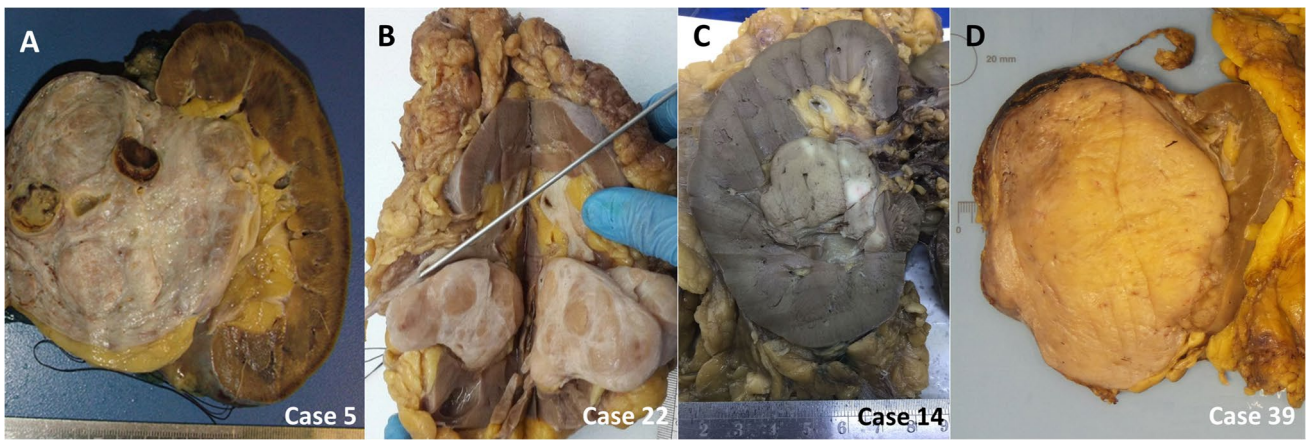


Fig. 3 Tumors are typically well-circumscribed with homogeneous, fibrillary, tan-white cut surfaces

"renal SFT". We also highlighted the usefulness of the Demicco risk stratification system in predicting prognosis, as well as PAX8 expression in a subset of renal SFT. Morphologically, two major histological patterns are present: 1) Fibrous pattern, which is "paucicellular" and collagenous, and 2) Cellular pattern, which shows storiform pattern with delicate vasculature. The presence of a third group of cases with mixed patterns in a significant number of instances suggests a morphological spectrum. Myxoid degeneration is another common finding, occurring in up to 40% of cases, particularly in association with cellular pattern. Less common features, such as tubular entrapment, minimally invasive borders, and vascular invasion, might lead to a false impression of increased malignant potential. In our study, however, minimal infiltrative borders, vascular invasion, or marginal excision with minimal surgical margin positivity do not appear to worsen the prognosis.

Designating SFT as benign or malignant is a traditional yet somewhat controversial approach, particularly following the introduction of 3-tier and 4-tier risk stratification

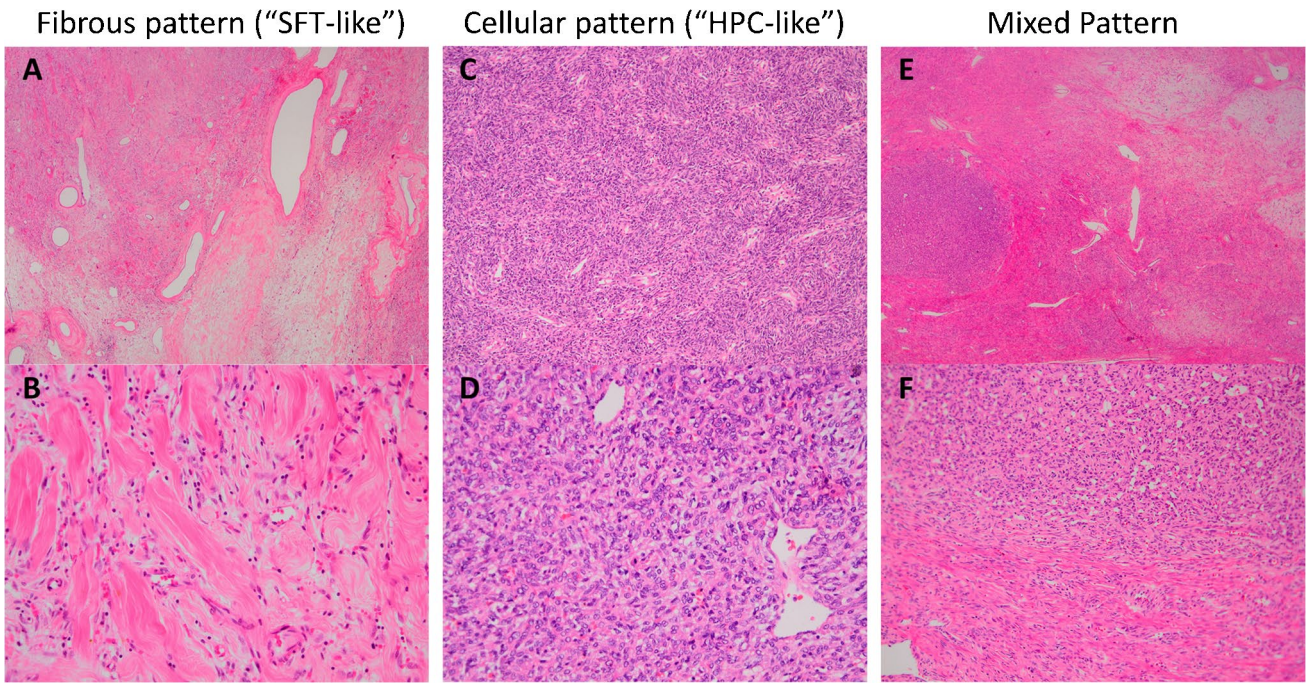


Fig. 4 Main morphological spectrum of the cases: **a**-**b**) Fibrous ("SFT-like") pattern with kelloidal collagen and hypocellularity (Case #5). **c**-**d**) Cellular ("HPC-like") pattern with short spindle cells in cartwheel formation, intermediate to high cellularity, staghorn vessels, and lack of collagen (Case #25). **e**–**f**) Mixed pattern showing both patterns (Case #24)

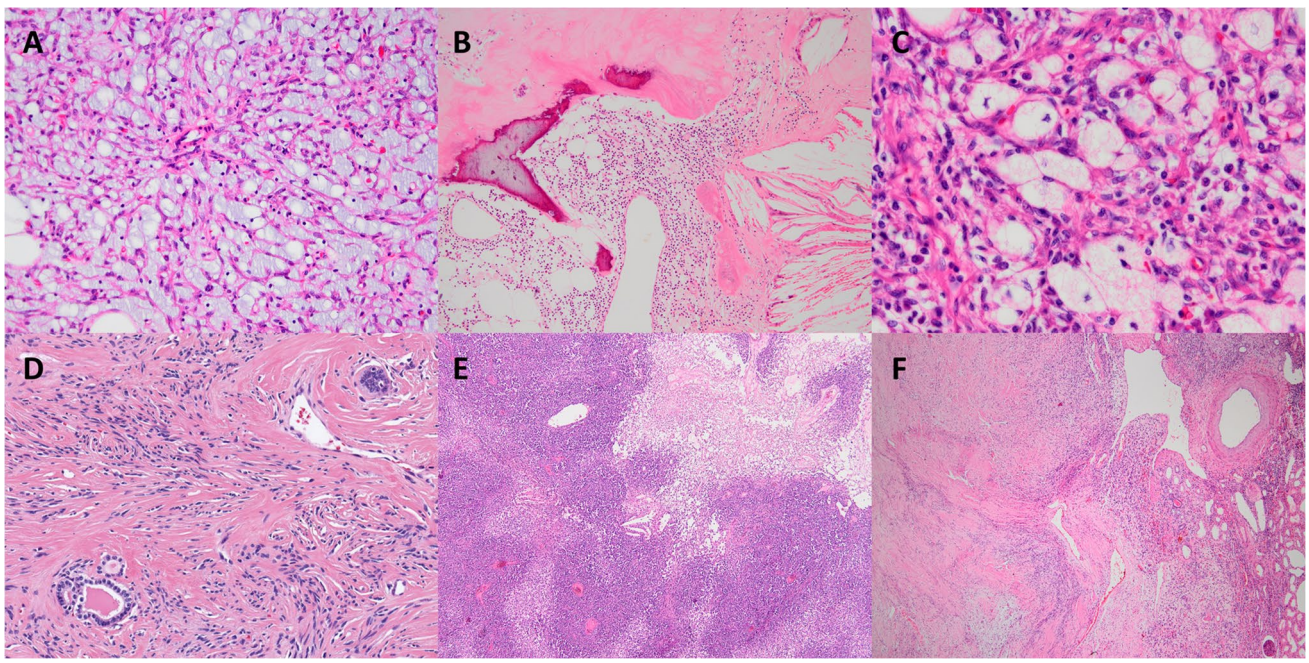


Fig. 5 Range of morphological findings in renal SFT: **a**) myxoid change (Case #7), **b**) bone metaplasia (Case #1), **c**) lipoblast-like cells (Case #7), **d**) renal tubular entrapment (Case #6), **e**) necrosis (Case #40), and **f**) vascular herniation to hilar veins (Case #22)

models [2]. The Demicco risk stratification system has been validated in SFT across many sites; however, renal SFT has not been studied due to its rarity, resulting in a lack of a substantial series [32, 33]. In this study, we acquired interesting observations when applying risk variables to renal SFT. For instance, necrosis was encountered in nine tumors:

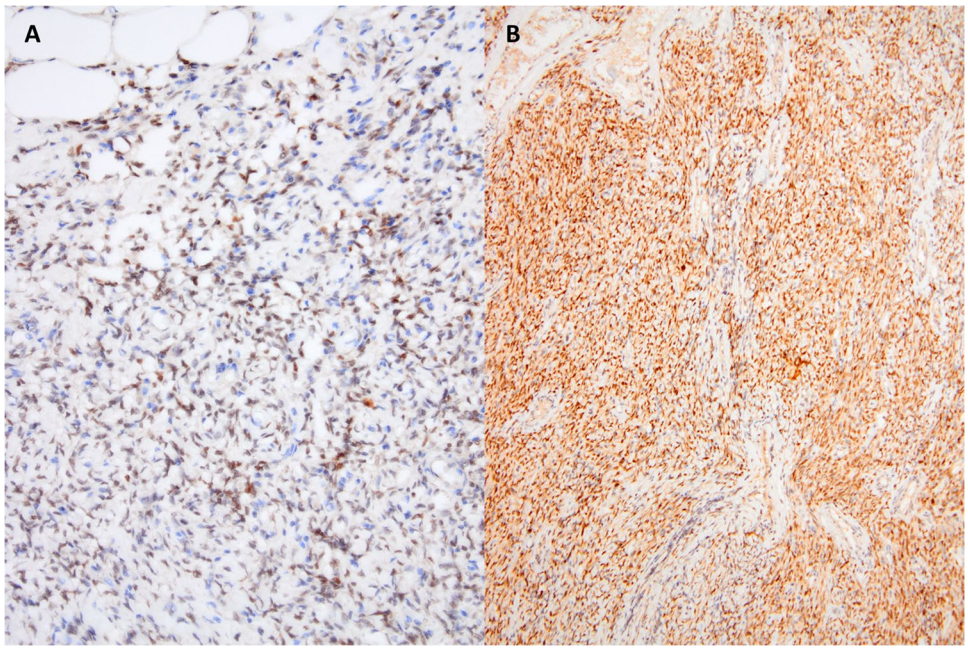


Fig. 6 Focal/patchy (**a**, case #22) or diffuse (**b**, case #15) STAT6 expression

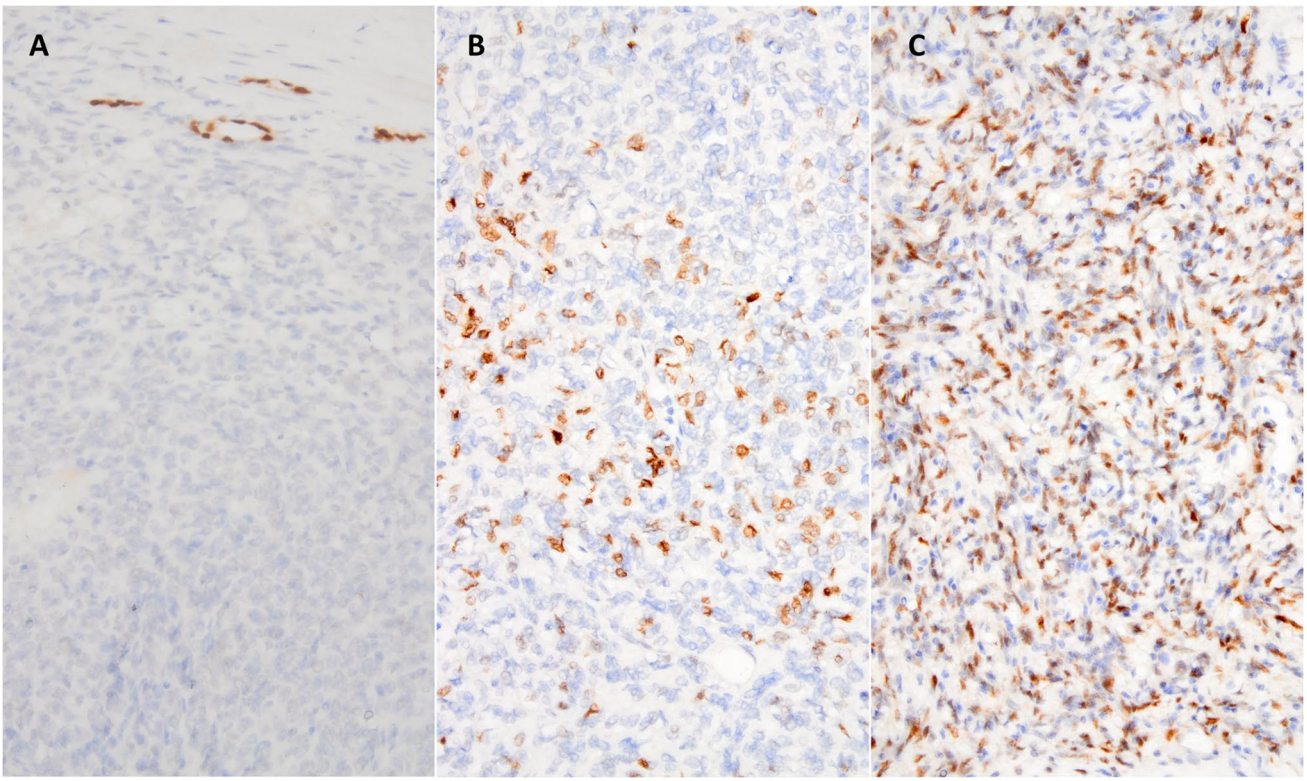


Fig. 7 Negative (**a**), focal (**b**), or diffuse (**c**) PAX8 expression in renal solitary fibrous tumor. Note the presence of normal tubules expressing PAX8 (**a**)

One low-, six intermediate-, and two high-risk tumors. Moreover, metastatic SFT was similarly present in low-, intermediate-, and high-risk categories. Despite necrosis and/or metastatic disease in all risk groups, the Demicco risk score still appears to predict prognosis reasonably well. For instance, a patient with metastatic SFT in the low-risk group was alive after a follow-up of 84 months, whereas both patients with metastatic SFT in the high-risk group

succumbed to the disease. It might mean that Demicco's risk stratification holds prognostic value even when the SFT is metastatic, but more cases with longer follow-up are needed.

Differential diagnosis of renal SFT includes renal cell carcinoma with sarcomatoid features, juxtaglomerular cell tumor, mixed stromal and epithelial tumor (mainly due to tubular entrapment), and other benign or malignant mesenchymal neoplasms such as angiomyolipoma, synovial sarcoma, leiomyosarcoma, dedifferentiated liposarcoma, sclerosing epithelioid fibrosarcoma, and myoepithelial-like neoplasms. In contrast to SFT, renal cell carcinoma with sarcomatoid features aggressively infiltrate surrounding tissue, display highly pleomorphic cytology, prominent necrosis, and commonly express keratins or EMA. Focal or diffuse PAX8 expression in SFT is identified in 27–43% of cases, particularly at the extrapleural locations [34, 35], and it may complicate distinguishing SFT from RCC. Previous studies utilized a polyclonal PAX8 antibody; we also observed that overall 20% of SFT were at least focally PAX8 positive, and PAX8 expression was present in 4 of 10 (40%) cases, even with monoclonal anti-PAX8 antibody.

Juxtaglomerular cell tumors are usually clinically symptomatic and are almost always located in the parenchyma, whereas renal SFT is typically found in the renal hilum. In a recent series of juxtaglomerular cell tumors, one misdiagnosed case was corrected as SFT, since both tumors are CD34-positive. However, STAT6 positivity and *NAB2::STAT6* rearrangement are specific for SFT, which also exhibits a distinct methylation profile [36]. In addition, strong GATA3 expression is consistently present in juxtaglomerular cell tumors [37]. Expression of STAT6 as a consequence of *STAT6* amplification is noted in a subset of dedifferentiated liposarcomas and in GLI1-amplified tumors, both may present in the kidney and hence mimic SFT.

Renal leiomyosarcoma originates in the renal veins, which are located in the hilum, similar to most SFTs. While they can display HPC pattern, these tumors are readily identifiable by their unique characteristics, including elongated, intersecting fascicles of spindle cells with eosinophilic cytoplasm and perinuclear hofs, in addition to the expression of smooth muscle markers. Renal synovial sarcoma closely resembles renal SFT morphologically; however, it lacks CD34 and STAT6 expression and is designated by keratin positivity and *SS18::SSX* rearrangement.

Our cohort of 43 cases included three renal SFT classified as lipomatous SFT, one of which even contained lipoblast-like cells. Fat-forming SFT is a well-known morphological variant of SFT [3] and has also been reported in the kidney [7, 38–40]. When such cells are found in a renal or pararenal mass, SFT should be considered in the differential diagnosis alongside well-differentiated or dedifferentiated liposarcoma and angiomyolipoma. This is especially critical when reviewing small biopsies, as the value of the STAT6 immunostain becomes increasingly evident; however, its positive expression is not exclusive to SFT. STAT6 expression is identified in a subset (10%) of dedifferentiated liposarcoma [41]. Therefore, the *MDM2* gene amplification status should be investigated, particularly in tumors exhibiting high-grade features and accompanying areas of well-differentiated liposarcoma. Another distinguishing feature is that STAT6 expression is found in the cytoplasm and nucleus of most dedifferentiated liposarcomas, while it is typically only present in the nucleus in SFT [42]. Fat-poor angiomyolipoma typically appears as exophytic masses composed of spindle-epithelioid cells with eosinophilic granular cytoplasm and thick-walled vessels, exhibiting a myomelanocytic immunophenotype.

STAT6 expression serves as a valuable and widely used surrogate for *NAB2::STAT6* rearrangement, the molecular signature of SFT [43]. In our study, all cases except one were STAT6 positive, with 10% showing focal or patchy expression. We primarily suggest that the loss or focal STAT6 expression results from the significant negative impact of late fixation on STAT6 staining. Similarly, in their seminal paper introducing STAT6 IHC, Doyle et al. stated that one of the tumors (2%) was negative for STAT6 and 7 of 60 cases (12%) exhibited heterogeneous staining with a zonal distribution pattern, particularly in the center of the tissue, which may be related to incomplete tissue fixation [43]. Furthermore, older paraffin blocks tend to show less STAT6 expression [42], which may explain STAT6 negativity in our one STAT6-negative renal SFT.

Limitations of this study include the retrospective nature of the observation. Moreover, the IHC work-up in different pathology laboratories exposed our study to varying staining performances. We did not perform the gold standard *NAB2::STAT6* fusion testing in our cases, although STAT6 is proven to be a reliable surrogate marker. The absence of BCOR expression profile in our cohort would also be considered a limitation since its expression is identified in particularly high-grade SFT [30].

In conclusion, our study highlights significant PAX8 expression in renal SFT and is the first one to systematically assess the utility of the risk stratification scheme in renal SFT.

Supplementary Information The online version contains supplementary material available at https://doi.org/10.1007/s00428-025-04264-6.

Author's contribution GG, MA, and KK designed the project. All authors contributed cases. GG, KK, and MA wrote the full manuscript draft. MA and KK created the figures. MA, KK, AA, KT, and PA revised the full manuscript.

Funding None.

Data Availability The datasets generated during and/or analyzed during the current study are not publicly available, but are available from the corresponding author upon reasonable request.

Declarations

In this retrospective study, all participating institutions contributed archival material under the approval of each institution's review board, and the completely de-identified information does not interfere with the patients' treatment.

Conflict of interest The authors did not receive support from any organization for the submitted work. The authors have no competing interests to declare that are relevant to the content of this article.

Disclaimer A part of this work was presented at the 33rd (Virtual) European Congress of Pathology, 29—31 August 2021 (ECP 2021). This manuscript is not under review elsewhere.

References

1. Chmielecki J, Crago AM, Rosenberg M, O'Connor R, Walker SR, Ambrogio L, Auclair D, McKenna A, Heinrich MC, Frank DA, Meyerson M (2013) Whole-exome sequencing identifies a recurrent NAB2-STAT6 fusion in solitary fibrous tumors. Nat Genet 45:131–132. https://doi.org/10.1038/ng.2522
2. Soft tissue and bone tumours (2020) WHO classification of tumours, vol 3, 5th edn. International Agency for Research on Cancer, Lyon
3. Soft tissue and bone tumours (2013) WHO classification of tumours, vol 2, 4th edn. International Agency for Research on Cancer, Lyon
4. Khater N, Khauli R, Shahait M, Degheili J, Khalifeh I, Aoun J (2013) Solitary fibrous tumors of the kidneys: presentation, evaluation, and treatment. Urol Int 91:373–383. https://doi.org/10.1159/000354394
5. Kuroda N, Ohe C, Sakaida N, Uemura Y, Inoue K, Nagashima Y, Hes O, Michal M (2014) Solitary fibrous tumor of the kidney with focus on clinical and pathobiological aspects. Int J Clin Exp Pathol 7:2737–2742
6. Wang H, Liao Q, Liao X, Wen G, Li Z, Lin C, Zhao L (2014) A huge malignant solitary fibrous tumor of kidney: case report and review of the literature. Diagn Pathol 9:13. https://doi.org/10.1186/1746-1596-9-13
7. Chen Y, Wang F, Han A (2015) Fat-forming solitary fibrous tumor of the kidney: a case report and literature review. Int J Clin Exp Pathol 8:8632–8635
8. Abeygunasekera AM, Ginige AP, Liyanage IS, Hareendra K (2015) A solitary fibrous tumor of the kidney. J Cancer Res Ther 11:662. https://doi.org/10.4103/0973-1482.138128
9. Cheung F, Talanki VR, Liu J, Davis JE, Waltzer WC, Corcoran AT (2016) Metachronous malignant solitary fibrous tumor of kidney: case report and review of literature. Urol Case Rep 4:45–47. https://doi.org/10.1016/j.eucr.2015.09.004
10. Nakajima R, Abe K, Kondo T, Nagashima Y, Kimura K, Fukushima K, Momose M, Kondo C, Tanabe K, Sakai S (2015) FDG-PET/CT and CT findings of a benign solitary fibrous tumor of the kidney; correlation with pathology. Asia Ocean J Nucl Med Biol 3:116–119
11. Chen X, Wang JF, Ding ZS, Zhou XF (2018) Solitary fibrous tumor of the kidney treated with laparoscopic partial nephrectomy: a case report. Chin Med Sci J 33:64–68. https://doi.org/10.24920/31803
12. Lalwani AK, Faiq SM, Ahuja J (2018) Solitary fibrous tumor of kidney. J Coll Physicians Surg Pak 28:564–565. https://doi.org/10.29271/jcpsp.2018.07.564
13. Fu W, Bing Q, JingJing Z, Lijian L, Zhibin X, Qijian D, Jiwen C (2019) Clinicopathological characteristics of renal solitary fibrous tumor: a single institution experience. Medicine (Baltimore) 98:e14618. https://doi.org/10.1097/md.0000000000014618
14. Zaghbib S, Chakroun M, Essid MA, Saadi A, Bouzouita A, Derouiche A, Slama MRB, Ayed H, Chebil M (2019) Solitary fibrous tumor of the kidney: a case report. Int J Surg Case Rep 62:112–114. https://doi.org/10.1016/j.ijscr.2019.08.004
15. De Luca L, Creta M, Barone B, Crocetto F, Cieri M, Campanino MR, Insabato L, Mangiapia F, Fusco F, Imbimbo C, Mirone V, Longo N (2020) A case of incidentally discovered solitary fibrous tumor of the kidney: A case study. Mol Clin Oncol 13:39. https://doi.org/10.3892/mco.2020.2109
16. Marcinek M, Majcherczyk K, Nowak M, Targonski A, Tkocz M (2021) Solitary fibrous tumor of the retroperitoneal space. Case Rep Surg 2021:8857274. https://doi.org/10.1155/2021/8857274
17. Zhang Q, Qin J, Li Y, Wu T (2019) Primary solitary fibrous tumor of kidney: a case report and literature review. Urol Case Rep 23:92–94. https://doi.org/10.1016/j.eucr.2019.01.012
18. Sammoud S, Ferjani S, Hamdani M, Toumi A (2019) Malignant renal solitary fibrous tumor with two local recurrences and distant pulmonary metastasis. Urology 127:9–12. https://doi.org/10.1016/j.urology.2019.01.029
19. Daly A, Dorman AM, Hinchion J (2019) Metastatic solitary fibrous tumour of the kidney presenting more than a decade later with pulmonary disease. Ir Med J 112:954
20. Usuba W, Sasaki H, Yoshie H, Kitajima K, Kudo H, Nakazawa R, Sato Y, Takagi M, Chikaraishi T (2016) Solitary fibrous tumor of the kidney developing local recurrence. Case Rep Urol 2016:2426874. https://doi.org/10.1155/2016/2426874
21. Bezerra ES, Andrighetto OP, Costa MVS, Chiarelli LO, Moleiro W, Schultz L (2018) Bilateral renal involvement by solitary fibrous tumor - report of a case in the post-WHO/2016 era. Urol Case Rep 17:7–9. https://doi.org/10.1016/j.eucr.2017.12.003
22. Zhao G, Li G, Han R (2012) Two malignant solitary fibrous tumors in one kidney: case report and review of the literature. Oncol Lett 4:993–995. https://doi.org/10.3892/ol.2012.858
23. Hertz AM, Childers CK, Wingate JT, Perry JT, Kitley CA, Brand TC, Anderson MI (2019) Malignant solitary fibrous tumor of the renal vein presenting as a giant renal artery aneurysm: a case report and review of literature. Int J Surg Pathol 27:72–76. https://doi.org/10.1177/1066896918787650
24. Almohammad F, Bakour MM (2021) Solitary fibrous renal tumor with thrombus extension into the inferior vena cava and right atrium. Asian Cardiovasc Thorac Ann. https://doi.org/10.1177/0218492321997391
25. Mearini E, Cochetti G, Barillaro F, Fatigoni S, Roila F (2014) Renal malignant solitary fibrous tumor with single lymph node involvement: report of unusual metastasis and review of the literature. Onco Targets Ther 7:679–685. https://doi.org/10.2147/ott.S51664
26. Khowaja A, Johnson-Rabbett B, Bantle J, Moheet A (2014) Hypoglycemia mediated by paraneoplastic production of insulin like growth factor-2 from a malignant renal solitary fibrous tumor - clinical case and literature review. BMC Endocr Disord 14:49. https://doi.org/10.1186/1472-6823-14-49
27. Ma J, Du J, Zhang Z, Wang H, Wang J (2014) Synchronous primary triple carcinoma of thyroid and kidney accompanied by solitary fibrous tumor of the kidney: a unique case report. Int J Clin Exp Pathol 7:4268–4273
28. Ichiyanagi O, Ito H, Takai S, Naito S, Kato T, Nagaoka A, Yamakawa M (2015) A GRIA2 and PAX8-positive renal solitary

fibrous tumor with NAB2-STAT6 gene fusion. Diagn Pathol 10:155. https://doi.org/10.1186/s13000-015-0386-x
29. Bellizzi AM (2020) An algorithmic immunohistochemical approach to define tumor type and assign site of origin. Adv Anat Pathol 27:114–163. https://doi.org/10.1097/PAP.0000000000000256
30. Argani P, Kao YC, Zhang L, Sung YS, Alaggio R, Swanson D, Matoso A, Dickson BC, Antonescu CR (2019) Bcor overexpression in renal malignant solitary fibrous tumors: a close mimic of clear cell sarcoma of kidney. Am J Surg Pathol 43:773–782. https://doi.org/10.1097/pas.0000000000001243
31. Conzo G, Tartaglia E, Gambardella C, Mauriello C, Esposito D, Mascolo M, Russo D, Stornaiuolo G, Gaeta GB, Santini L (2014) Suprarenal solitary fibrous tumor associated with a NF1 gene mutation mimicking a kidney neoplasm: implications for surgical management. World J Surg Oncol 12:87. https://doi.org/10.1186/1477-7819-12-87
32. Demicco EG, Wagner MJ, Maki RG, Gupta V, Iofin I, Lazar AJ, Wang WL (2017) Risk assessment in solitary fibrous tumors: validation and refinement of a risk stratification model. Mod Pathol 30:1433–1442. https://doi.org/10.1038/modpathol.2017.54
33. Demicco EG, Park MS, Araujo DM, Fox PS, Bassett RL, Pollock RE, Lazar AJ, Wang WL (2012) Solitary fibrous tumor: a clinicopathological study of 110 cases and proposed risk assessment model. Mod Pathol 25:1298–1306. https://doi.org/10.1038/modpathol.2012.83
34. McDaniel AS, Palanisamy N, Smith SC, Robinson DR, Wu YM, Chinnaiyan AM, McHugh JB, Greenson JK, Kunju LP (2016) A subset of solitary fibrous tumors express nuclear PAX8 and PAX2: a potential diagnostic pitfall. Histol Histopathol 31:223–230. https://doi.org/10.14670/hh-11-670
35. Ullman D, Gordetsky J, Siegal GP, Prieto-Granada CN, Wei S, Stevens TM (2019) PAX8 expression in solitary fibrous tumor: a potential diagnostic pitfall. Appl Immunohistochem Mol Morphol 27:195–202. https://doi.org/10.1097/pai.0000000000000561
36. Michalova K, Martinek P, Mezencev R, Gupta S, Williamson S, Wasco M, Mohanty S, Magi-Galluzzi C, Canete-Portillo S, Aron M, Kandukuri S, Lobo J, Barkan GA, Kilic I, Strakova-Peterikova A, Pivovarcikova K, Michal M, Michal M, Ulbright TM, Acosta AM (2025) Renal juxtaglomerular cell tumors exhibit distinct genomic and epigenomic features and lack recurrent gene fusions: comprehensive molecular analysis of a multi-institutional series. Am J Surg Pathol 49:217–226. https://doi.org/10.1097/PAS.0000000000002344
37. Gupta S, Folpe AL, Torres-Mora J, Reuter VE, Zuckerman JE, Falk N, Stanton ML, Muthusamy S, Smith SC, Sharma V, Sethi S, Herrera-Hernandez L, Jimenez RE, Cheville JC (2022) Immunohistochemical expression of renin and GATA3 help distinguish juxtaglomerular cell tumors from renal glomus tumors. Hum Pathol 128:110–123. https://doi.org/10.1016/j.humpath.2022.07.016
38. Yamaguchi T, Takimoto T, Yamashita T, Kitahara S, Omura M, Ueda Y (2005) Fat-containing variant of solitary fibrous tumor (lipomatous hemangiopericytoma) arising on surface of kidney. Urology 65:175. https://doi.org/10.1016/j.urology.2004.08.011
39. Cortes LG, Caserta NM, Billis A (2014) Fat-forming solitary fibrous tumor of the kidney: a case report. Anal Quant Cytopathol Histopathol 36:295–298
40. Bacalbasa N, Balescu I, Jinescu G, Marcu M, Contolenco A, Pop D, Dobritoiu D, Ionescu O, Ionescu P, Stoica C (2018) Fat-forming solitary fibrous tumor of the kidney - a case report and literature review. In Vivo 32:649–652. https://doi.org/10.21873/invivo.11288
41. Doyle LA, Tao D, Mariño-Enríquez A (2014) STAT6 is amplified in a subset of dedifferentiated liposarcoma. Mod Pathol 27:1231–1237. https://doi.org/10.1038/modpathol.2013.247
42. Demicco EG, Harms PW, Patel RM, Smith SC, Ingram D, Torres K, Carskadon SL, Camelo-Piragua S, McHugh JB, Siddiqui J, Palanisamy N, Lucas DR, Lazar AJ, Wang WL (2015) Extensive survey of STAT6 expression in a large series of mesenchymal tumors. Am J Clin Pathol 143:672–682. https://doi.org/10.1309/AJCPN25NJTOUNPNF
43. Doyle LA, Vivero M, Fletcher CD, Mertens F, Hornick JL (2014) Nuclear expression of STAT6 distinguishes solitary fibrous tumor from histologic mimics. Mod Pathol 27:390–395. https://doi.org/10.1038/modpathol.2013.164

Publisher's Note Springer Nature remains neutral with regard to jurisdictional claims in published maps and institutional affiliations.

Springer Nature or its licensor (e.g. a society or other partner) holds exclusive rights to this article under a publishing agreement with the author(s) or other rightsholder(s); author self-archiving of the accepted manuscript version of this article is solely governed by the terms of such publishing agreement and applicable law.

Authors and Affiliations

Güneş Güner[1] · Mahmut Akgul[2] · Michael Michal[3,4] · Asli Yilmaz[5] · Buşra Yaprak Bayrak[6] · Bermal Hasbay[7] · Aylin Yazgan[8] · Nilüfer Kandemir[8] · Murat Oktay[9] · Deniz Bayçelebi[10] · Arkar Htoo[11] · Jose Lopez[12] · Ondrej Hes[4] · Arndt Hartmann[15] · Dilek E. Baydar[13] · Kril Trpkov[5] · Sambit K. Mohanty[14] · Abbas Agaimy[15] · Pedram Argani[16] · Kemal Kösemehmetoğlu[1]

✉ Kemal Kösemehmetoğlu
dokemal@hotmail.com;
Kemal.kosemehmetoglu@hacettepe.edu.tr

[1] Department of Pathology, Hacettepe University School of Medicine, Ankara, Türkiye

[2] Department of Pathology, Brigham and Women's Hospital, Boston, MA, USA

[3] Department of Pathology, Faculty of Medicine, Charles University, Plzen, Czech Republic

[4] Biopticka Laborator, Plzen, Czech Republic

[5] Department of Diagnostic and Molecular Pathology, Cumming School of Medicine, University of Calgary, Calgary, AB, Canada

[6] Department of Pathology, Kocaeli University School of Medicine, Kocaeli, Türkiye

[7] Department of Pathology, Adana Dr. Turgut Noyan Application and Research Center, Başkent University Faculty of Medicine, Adana, Türkiye

[8] Department of Pathology, Ankara Bilkent City Hospital, Ankara, Türkiye

[9] Department of Pathology, Memorial Hospital, Istanbul, Türkiye

[10] Department of Pathology, Ondokuz Mayıs University School of Medicine, Samsun, Türkiye

[11] Department of Pathology, Montefiore Medical Center, New York City, NY, USA

[12] Department of Pathology, Cruces U. Hospital, Biocruces Institute, University of the Basque Country, Barakaldo, Spain

[13] Department of Pathology, Koç University School of Medicine, Istanbul, Türkiye

[14] Core Diagnostics, Gurgaon, India

[15] Institute of Pathology, University of Erlangen-Nuremberg, Erlangen, Germany

[16] Department of Pathology, Johns Hopkins University, Baltimore, MD, USA